AIAA JOURNAL
Vol. 34, No. 3, March 1996

Planar OH Density and Apparent Temperature Measurements in a Supersonic Combusting Flow

G. Laufer,* T. M. Quagliaroli,† R. H. Krauss,‡ R. B. Whitehurst III,§ and J. C. McDaniel¶
University of Virginia, Charlottesville, Virginia 22903
and
J. H. Grinstead**
Princeton University, Princeton, New Jersey 08544

Distributions of the absolute density of OH and of the population densities of five OH rotational states were obtained in a supersonic H_2–air combustion tunnel using planar laser-induced fluorescence. A tunable KrF excimer laser was used to excite, nonsimultaneously, the five separate ro-vibronic lines in the (3–0) vibrational band of OH. Measurements were calibrated against measurements in an atmospheric air furnace, where known quantities of OH are formed by the thermal dissociation of H_2O molecules. Despite flame intermittency, a sum of each of these nonsimultaneous measurements represents the time-averaged population density of the probed state. Present results show that these time-averaged measurements of the populations of the probed states still follow a Boltzmann distribution. Therefore, measurements of the average population of any pair of states can provide the two independent average properties required to define the average thermodynamic state of OH.

Introduction

THE validation of numerical codes that simulate turbulent or supersonic reacting flows requires nonintrusive measurements of thermodynamic flow properties such as temperature and species concentration. For example, in some supersonic combustion tests the temperature and Mach number exceed 3000 K and $M = 2$, respectively. Clearly physical probes are unlikely to survive the conditions of such flows, and nonintrusive techniques must be used instead. Optical nonintrusive diagnostic techniques have been shown to provide the measurement accuracy and spatial resolution needed to produce benchmark data sets for these validations. In particular, planar laser-induced fluorescence (PLIF) has evolved from a qualitative flowfield visualization technique to a quantitative, planar, multicomponent measurement tool. This method has been successfully applied to a variety of experimental situations involving both nonreacting[1] and reacting[2] fluid flow. PLIF measurements involving naturally occurring molecular species, such as O_2 (Ref. 3), NO (Ref. 4), and OH, have supplied two-dimensional species concentration,[5] temperature,[5,6] and velocity[5] data in turbulent flows.

Generally, to obtain two independent thermodynamic properties, such as the density of the OH radical and its temperature, at least two independent measurements are required. Two PLIF measurements are independent when two different transitions originating at two different states are excited. Since the fluorescence intensities of PLIF are related to the densities of the probed states, when the gas is in thermodynamic equilibrium the two independent laser-induced fluorescence (LIF) measurements can be used to determine the population distribution among the states of the probed species. By assuming that the internal energy distribution is thermally equilibrated with the transnational energy, both the gas-kinetic temperature and the species density can be determined from the two fluorescence measurements. Ideally, these two measurements should be performed by simultaneously using two laser systems for the excitation and two detection systems to record the fluorescence.[7] With such simultaneous measurements the signal of both LIF tests is assured to emanate from the same gas sample. Alternatively, a single laser may be used for both measurements by tuning it first to coincide with one absorption line and then to the excitation of the second transition. However, in fast or highly turbulent flows, the time between these two measurements may exceed the time required by a fluid element to pass through the probe volume. Therefore, by the time the second laser pulse is available for the measurement, the fluid in the probe volume may be replaced by a potentially uncorrelated fluid element. For measurements that depend linearly on the fluorescence emission, e.g., density, simple averaging may be used to correct for flow property fluctuations between laser pulses. However, for temperature, which depends exponentially on the induced fluorescence intensity, algebraic averaging of the fluorescence fluctuations that are induced by flow property fluctuations between two consecutive laser pulses may introduce significant systematic errors. Nevertheless, previous results[8,9] demonstrate that if the flow fluctuations are relatively small, the systematic error introduced by two nonsimultaneous measurements may be acceptable.

The present work investigates the flowfield within a model H_2–air scramjet combustor using quantitative OH PLIF imaging. Since only one laser was available, the measurement of two independent thermodynamic properties of OH required the use of two nonsimultaneous laser pulses. A tunable KrF laser, emitting nominally at 248 nm, was used to excite five ro-vibronic transitions within the $A^2\Sigma^+(v' = 3) \leftarrow X^2\Pi(v'' = 0)$ band of OH. The population density fields of the probed rotational levels of OH were obtained from nonsimultaneous, multiline, time-averaged fluorescence images. The distributions of these quantities were mapped in the highly turbulent, supersonic flame region downstream of an unswept-ramp injector. From these results, the distributions of the OH density and an apparent temperature were extracted. Although the temperature distributions acquired from two or more time-averaged, nonsimultaneous, fluorescence measurements in this highly turbulent field may not represent the true average temperature of the postflame gases, it was shown here to be representative of the average rotational distribution of OH. These averaged state populations are nevertheless valid independent thermodynamic properties of OH that can be used to specify the thermodynamic state of this species

Presented as Paper 95-0512 at the AIAA 33rd Aerospace Sciences Meeting, Reno, NV, Jan. 10–12, 1995; received Feb. 9, 1995; revision received Oct. 3, 1995; accepted for publication Dec. 5, 1995.

*Associate Professor, Aerospace Research Laboratory, 570 Edgemont Road. Senior Member AIAA.
†Research Assistant, Aerospace Research Laboratory, 570 Edgemont Road. Student Member AIAA.
‡Research Associate Professor, Aerospace Research Laboratory, 570 Edgemont Road. Member AIAA.
§Research Engineer, Aerospace Research Laboratory, 570 Edgemont Road.
¶Professor, Aerospace Research Laboratory, 570 Edgemont Road. Member AIAA.
**Research Associate, Department of Mechanical and Aerospace Engineering. Member AIAA.

in turbulent reacting flows. The results of the present measurement of the rotational distribution is termed here as the apparent temperature T_{app} to distinguish it from the true, instantaneously measured temperature T.

Theoretical Background

In a typical LIF experiment, molecules are selectively excited from a single rotational state to an excited energy level by narrowband radiation that is resonant with that specific absorption transition. Once excited, molecules may dispose of their energy by either exchanging it collisionally with other molecules, by dissociation, or by spontaneous emission. By detecting this spontaneous emission selectively and measuring its extent, the population of the excited state and hence the population of the probed rotational state may be determined. For planar imaging, the fluorescence is recorded by a charge-coupled device (CCD) camera through an array of filters that are designed to reject radiation from all sources, including elastic scattering of the laser radiation, while transmitting the fluorescence emitted by the excited molecules. The equation for the signal that is detected by one pixel of a camera with n_p rows and m_p columns of pixels when imaging a section with a length of L along the laser beam was previously presented[10] in terms of photoelectrons n_{pe}:

$$n_{pe} = \eta N_{OH} \beta(T) \times \sigma_{12} \left[\frac{E_L g(N,T)}{n_p h \nu_{12}} \right] \left(\frac{L}{m_p} \right) \left(\frac{A_{2f}}{A_{ef} + Q_{21} + P_2} \right) \quad (1)$$

where η is the fraction of the total number of emitted photons that contribute to the electronic signal of each pixel, N_{OH} is the number density of OH, σ_{12} is the absorption cross section, $E_L/n_p h\nu_{12}$ is the number of incident laser photons with nominal frequency ν_{12} traveling along the strip that is imaged by one row of pixels, where E_L is the pulse energy, and $g(N, T)$ is the density N and temperature-dependent overlap integral between the absorption and laser line shapes, L/m_p is the length of the segment that is imaged by a single pixel, A_{2f} is the Einstein A coefficient of the detected transition, $A_{ef} = \Sigma A_{2i}$ is the total rate of spontaneous emission from the excited state obtained by the summation of the Einstein A coefficients of all the allowed transitions from the excited state, Q_{12} is the rate of collisional quenching, and P_2 is the predissociation rate of the excited level. When the bandwidth of the laser is broad relative to the absorption bandwidth, as in the present experiment, $E_L g(N, T)$, which is the fraction of the laser energy that is absorbed by the absorption line, is relatively insensitive to fluctuations in gas density and temperature. The function $\beta(T)$ is the population fraction of the absorbing state, which at conditions of thermodynamic equilibrium at a temperature T is proportional to

$$\beta(T) \propto [g_i/Q(T)] \exp[-(E_i/kT)] \quad (2)$$

where g_i and E_i are the degeneracy and energy of the probed-state, respectively, $Q(T)$ is the temperature-dependent partition function, and k is the Boltzmann constant.

Although the LIF signal is predicted by Eq. (1) to increase linearly with N_{OH} and exponentially with T, the dependence may be complicated by Q_{21}, which depends on the temperature and the density of other species in the flow such at H_2O and N_2. For example, the collisional quenching rate of OH in 30% water-vapor-air mixture at 1 atm and 2000 K is found using a term given by Ref. 11 to be $Q_{12} = 5.76 \times 10^8\ s^{-1}$. For comparison the Einstein A coefficient for a $P_1(8)$ emission in the 3–0 band of OH is $A_{2f} = 1.984 \times 10^5\ s^{-1}$ (Ref. 12). Clearly, when predissociation is negligible, the LIF measurement strongly depends on the thermodynamic properties of the collisional partners of the probed specie. However, for excitation of the (3–0) band of OH, the rate of predissociation is significantly larger than both Q_{12} and A_{2f}. For example, for the excitation of the $P_1(8)$ rotational line, the predissociation rate is $P_2 = 0.83 \times 10^{10}\ s^{-1}$ (Ref. 13). Therefore, A_{ef} and Q_{12} in the denominator of Eq. (1) are negligible relative to P, thereby rendering the OH fluorescence yield from that state relatively free from the effects of collisional quenching.[14] For the conditions of the present experiment, collisional quenching is negligible and the LIF emission is expected accordingly to be proportional to N_{OH} and to the relative occupational density of the probed state $\beta(T)$. In addition, the signal n_{pe} is proportional to the incident laser energy E_L that is spectrally coincident with the absorption line. The linear relationship between the LIF signal and the occupational density of each state and the incident laser energy allows the average population densities of individual states to be determined from measurements of time-averaged fluorescence signals, time-averaged laser energies, and time-averaged laser spectral distribution. Since each LIF measurement depends both on the temperature and the total density of the probed species, neither of these properties can be determined from a single LIF measurement. However, in exceptional cases it is possible to identify certain rotational states where the population is only weakly dependent on temperature. Although this weak dependance is limited to a finite range of temperatures, measurement of the LIF signal induced by the excitation of one of these states may serve for density measurements with an acceptable error by probing only a single transition.

Although measurement of OH density by the excitation of a single line may be possible, the fluorescence signal is a complex function of the characteristics of the laser system and of the collection optics, of the extent of the overlap between the laser and the absorption line shapes, and of the spectroscopic properties of OH, such as the absorption linewidths. The effect of these parameters is introduced implicitly into Eq. (1) by the coefficient η, by E_L, and by $g(N, T)$. To calibrate the magnitude of these parameters, an independent PLIF measurement of N_{OH} in a calibrated OH source must be obtained. The calibration source consisted of atmospheric air heated electrically in a furnace with three small openings for optical and atmospheric access. The OH fluorescence in this noncombusting environment has been shown to result from thermal dissociation of the naturally present water vapor.[15] Since the pressure, temperature, and H_2O concentration within the furnace are known, the OH concentration can be calculated via the law of mass action. A direct relationship between LIF yield and OH density can then be determined. The calibration coefficient combines the effect of uncertainties in the reported spectroscopic constants of OH,[11–13] optical and geometrical parameters of the system, laser beam parameters such as linewidth or locking efficiency, and, when the laser linewidth is broad relative to the absorption bandwidth (as here), the effect of the overlap integral $g(N, T)$. Using the results of the calibration test and the optical and geometrical parameters of both the calibration and experimental measurements, N_{OH} can be determined from the experimental photon count per unit laser energy.

Unlike density measurements that can be obtained by the excitation of a single judicially selected rotational transition, temperature measurements depend on the measurement of the fluorescence signals from at least two absorption transitions from two different states. If the fluorescence signals of these two LIF measurements are n_{pe1} and n_{pe2}, their ratio would be

$$R = \frac{n_{pe1}}{n_{pe2}} = C \frac{N_{OH1}}{N_{OH2}} \exp\left(-\frac{\Delta E_{12}}{kT} \right) \quad (3)$$

where C includes all of the spectroscopic parameters of the absorbing and emitting transitions including their degeneracies, N_{OH1} is the density of OH at the time of the first measurement, N_{OH2} is the density of OH at the time of the second measurement, and ΔE_{12} is the difference between the energy of the state probed by the first measurement and the energy of the state probed by the second measurement. For an incident laser with a bandwidth that is significantly broader than the absorption linewidth, the ratio R is independent of the laser parameters as well as the parameters of the collection system.

When the two LIF measurements that are used to determine R are simultaneous or when the fluctuations in OH density between the two measurements are small, $N_{OH1} = N_{OH2}$ and the ratio R depends only on the gas temperature. Thus, in these ideal conditions R may be used to determine the gas temperature with errors that depend only on the statistical nature of photon detection.[7] However, in highly turbulent flows or when the flame is intermittent, $N_{OH1} \neq N_{OH2}$. Since in such flows random cells of unmixed fuel or cool gases can reduce significantly the density of OH, thereby causing instances of

little or no signal at a point, the ratio R can no longer be assumed as being free of the OH density dependance. Furthermore, because of the nonlinear dependence of the Boltzmann fraction on temperature, the ratio obtained by nonsimultaneous fluorescence measurements of two energy levels may not yield the same temperatures that would be obtained from instantaneous, simultaneous measurements of the LIF of the same two states.

Although the temperature of intermittent or highly fluctuating flows may not be determined reliably from two (or more) nonsimultaneous LIF measurements, each time-averaged measurement represents the time-averaged population density of one quantum state. Repeating this measurement for other quantum states can be used to reproduce the time-averaged population distribution within an entire manifold of states. Under conditions of thermodynamic equilibrium—the same condition that is required for any temperature measurement—this measured population distribution may then be used to determine the specific internal energy or specific enthalpy of the gas. Together with the density that can be measured by the excitation of a temperature-insensitive rotational transition, the specific internal energy (or enthalpy) can specify an averaged thermodynamic state of the probed specie. Thus, although the average population densities of two quantum states may not be used to determine an average temperature, they by themselves represent two valid independent thermodynamic properties such as density and specific energy (or enthalpy), in the same manner as the instantaneous thermodynamic state is quantified by instantaneously measured properties.

To demonstrate this concept, a continuous-burn, supersonic, H_2–air combustion test facility that allows sufficient experimental run time was used to collect fluorescence and background images for five different absorption transitions at several stations in the flame region. Owing to the high intermittency of the flame, temperatures that are derived from time-averaged quantities are likely to be different from the true thermodynamic temperature. However, since the average population density of the ro-vibronic state is directly proportional to the average fluorescence collected from multiple measurements, these measurements may still be used to thermodynamically characterize the flow.

Experimental Apparatus and Procedure

Planar OH LIF images were obtained in a continuous flow, electrical-resistance heated, high-enthalpy, hydrogen–air combustion tunnel. Details of the facility are described elsewhere.[16] Heated supersonic airflow entered a model scramjet combustor with a 2.5 × 3.8 cm constant area at a nominal Mach number of $M = 2$. Hydrogen heated to 458 K was injected at a Mach number of $M = 1.7$ from a circular injector of diameter $D = 0.254$ cm. Fuel injection was normal to the base of a 10-deg unswept compression ramp and parallel to the ramp face. The base height was 0.635 cm and a width of 1.27 cm. For optical access, three uv-grade fused silica windows were mounted flush to the sides of the duct. The two side windows permitted laser beam entry and exit, and an observation window on the wall opposite to the ramp injector allowed imaging of the flame region downstream from the ramp base to a distance of approximately 38 injector diameters. A schematic

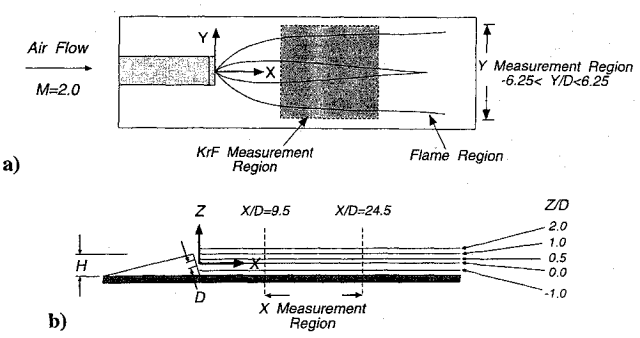

Fig. 1 Schematic diagram showing a) a top view of the test section through the observation window and b) side view of the same region where the location of the imaged planes is depicted.

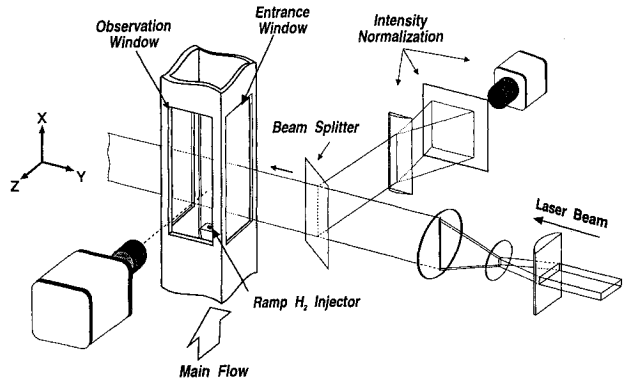

Fig. 2 Schematic diagram of the optical path of the PLIF system.

of the test section is shown in Fig. 1. The area that was illuminated by the laser sheet is marked in the top-view figure (Fig. 1a) by the shaded rectangle together with its dimensions relative to the injector diameter D. In addition, the locations of the planes of the five images are marked relative to the fuel injector wall by the lines in the side view (Fig. 1b). Since the origin of the coordinate system was located at the injector exit, negative values of the vertical coordinate z represent planes that are located between the injector and the injector wall.

The OH fluorescence was induced in this experiment by a tunable narrowband KrF laser, emitting nominally at 248 nm and at a bandwidth of approximately 0.8 cm^{-1}. For comparison, the absorption line width at 1 atm and 2000 K is 0.32 cm^{-1}. Using an automated tuning system, the laser could be tuned to resonance with selected rotational transitions within the $A^2\Sigma^+(v' = 3) \leftarrow X^2\Pi(v'' = 0)$ band of OH. The illumination and detection configuration is shown in Fig. 2. The laser energy at the test section was approximately 60 mJ/pulse and the beam was shaped into a 4.5 × 0.02 cm sheet. To identify the peak of the selected OH absorption line, a fraction of the laser beam was focused into a propane–air flame, and the subsequent OH fluorescence induced by the laser was monitored by a photomultiplier tube (PMT) equipped with a Schott UG-11 glass filter and a bandpass filter centered at 297 nm. These filters were selected to transmit OH fluorescence emitted in the $^2\Sigma^+(v' = 3) \rightarrow {}^2\Pi(v'' = 2)$ band while rejecting competing fluorescence from other combustion species and elastically scattered laser radiation. By tuning the laser and monitoring the signal detected by this PMT, the absorption peak of desired transitions could be identified. The fluorescence induced by the laser in the combustor test section was collected perpendicular to the laser sheet by a uv-transparent 105 mm f 4.5 lens, at a distance of 38.5 cm, and recorded using a uv-intensified and gated 576 × 384 array CCD camera. The overall pixel resolution of this configuration was approximately 0.2 mm. Also for this detection the desired fluorescence in the $^2\Sigma^+(v' = 3) \rightarrow {}^2\Pi(v'' = 2)$ band of OH was selectively transmitted by 10-nm narrow-bandpass filter, centered at 297 nm, and a Schott UG-11 glass filter, while discriminating against background emission by chemical luminescence and scattered laser light.

To allow selection of image planes, the sheet forming optics and the CCD camera were mounted on synchronized translation stages that maintained a constant spacing between the camera and the laser sheet, thereby assuring that the image remains focused throughout the experiment. Images were typically obtained at a 1.0-mm spacing, starting at the injector wall and extending to two ramp heights into the flame region. All PLIF images were corrected for the nonuniform response of the camera array by dividing them pixel by pixel by a flat-field distribution, obtained by imaging broadband uv light scattered from a uniform surface. To correct for the spatial laser intensity distribution, a portion of the laser sheet consisting of 4% of its energy was split just before the combustor and was projected onto a frosted glass screen. The profile of this sheet was imaged by a separate CCD camera. Single shot images showed that the pulse-to-pulse variations in laser energy at any point in the sheet were less than a few percent. Therefore, time-averaged images of this profile could be used reliably to correct for nonuniform spatial laser intensity distribution. To spatially correlate this time-averaged spatial

intensity array with the PLIF images recorded in the combustor, a pair of 0.5-mm wires were placed at the top and bottom of the laser sheet. The wires cast thin shadows in both the fluorescence and reference sheet images. Image processing software was used to crop the fluorescence images at the registration marks and divide each row in the PLIF images with the corresponding pixel in the one-dimensional intensity profile. Cropping the images slightly reduced the size of the imaged region, giving a usable image length of $15D$. To correct for background illumination that could not be removed by the filters, each PLIF measurement was repeated twice: once with the laser tuned to the peak of the absorption line and then with the laser tuned away from resonance with either OH or ambient O_2. The difference between these two images represented the net contribution by OH fluorescence.

Finally, to correlate these LIF measurements with the actual OH population density in each of the probed states, a separate calibration was performed by measuring the OH LIF signal in an atmospheric air furnace maintained at a temperature of 1800 K.[15] The OH LIF measurements in the furnace were performed with the same laser and detection system that were used in the combustion tunnel. Therefore, the relationship between the signal measured in the furnace in terms of counts per CCD array pixel and between the known OH population density in each of the probed states could be used to scale the fluorescence measurements in the combustion tunnel to obtain the population density in each of the probed states there. This scaling was automatically performed for each PLIF image by the same software used to correct the images for laser power variation.

To obtain apparent temperature fields, images of the time-averaged fluorescence intensity induced by the excitation of five rotational lines—$P_1(8)$, $P_2(8)$, $Q_2(10)$, $Q_1(11)$, and $Q_2(11)$—were used pixel by pixel to calculate the Boltzmann distribution at each point. Although the apparent temperature at each point was usually calculated by using all five fluorescence values, if the average fluorescence value of a spectral line at a point was lower than 10% of the peak intensity recorded for that spectral line elsewhere in that image, the value was discounted from the temperature calculation at that point. Thus, the apparent temperatures of several points were obtained by using fewer than five fluorescence measurements.

Results and Discussion

A set of measured OH concentration distributions is shown in Fig. 3. For these measurements, the main flow entered the combustor with freestream Mach number of 2.07, a stagnation pressure of 308 kPa, and a stagnation temperature of 1200 K. The injector delivered H_2 to the main airflow at stagnation pressure and temperature of 757 kPa and 458 K, respectively. A fuel flow rate of 1.41 g/s provided an overall equivalence ratio of $\Phi \cong 0.21$. These fluorescence images are the average of 200 laser pulses, followed by background subtraction and normalization for spatial laser intensity variation. The origin of the coordinate system for these images is located at the center of the injector (Fig. 1). The five density fields are at distances Z/D of -1.0, 0.0, 0.5, 1.0, and 2.0 from the centerline of the injector, with the injector wall located at $Z/D = -1.6$. The direction of the main flow was parallel to the X axis. The laser sheet, which was parallel to the injector block, entered the test section along the Y direction. The detection orientation was parallel to the Z axis. The imaged region, as shown in Fig. 1, starts downstream of the ramp and covers a section of the reaction zone that was judged to be the most involved. Although the region near the base of the ramp contained a small recirculation zone, the flame that was attached to the ramp was observed to be quite narrow and was therefore excluded from the image. These OH density distributions were obtained by the excitation of the $Q_2(11)$ absorption transition. Although the variation in state population of the $N = 11$ level is at most 30% over a temperature range from 1500 to 3000 K, the choice of this transition was predicated by the absence of any competing O_2 transitions. This permitted accurate calibration in the furnace and interference-free combustion measurements. The density distributions were calculated from the LIF measurements assuming a uniform flame temperature of 1800 K. With this selection, the uncorrected error due to flame temperature fluctuations within a 1500–3000 K range were minimized to less than ±15%. In addition, the calibration measurement has been shown to introduce a further 6% uncertainty,[15] mostly due to the uncertainty in determining the relative humidity within the furnace. These two uncertainties, when combined, result in a total measurement uncertainty of ≤21%.

A potential error in these measurements due to electronic quenching by H_2O and by vibrational energy transfer by N_2 have been assessed using published quenching rates[17] and predissociation rates.[13] The loss of excited population by electronic quenching by water vapor in a 0.5-atm and 1800-K H_2–air flame, where the concentration of H_2 is 20% of the stoichiometric ratio, would cause <1% loss in the fluorescence quantum yield. Vibrational energy transfer (VET) may also introduce an error. One of the most efficient and abundant vibrational quenching partners in H_2–air flames is nitrogen.[18] In this experiment VET by N_2 may account for ~1% loss of the $v' = 3$ population. However, similar uncorrected quenching by N_2 within the atmospheric calibration source is likely to offset the uncorrected error introduced by VET in the flame. Therefore the total error in OH density measurements in this experiment is introduced only by collisional quenching by H_2O, which is expected to be ≤1%.

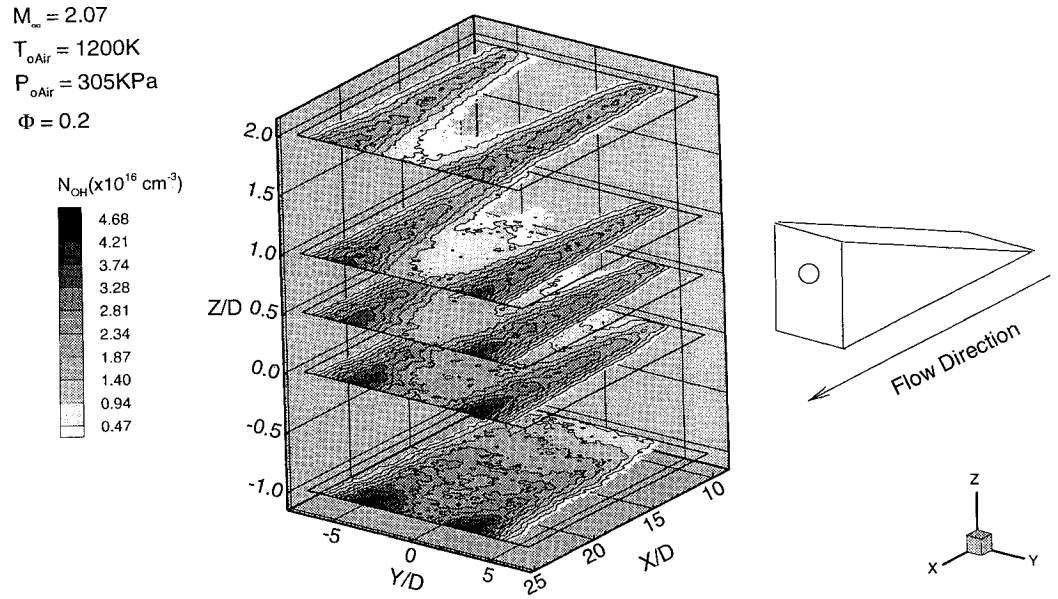

Fig. 3 Absolute OH concentration distributions for H_2 injection behind an unswept ramp. A schematic of the ramp was included for clarity and does not represent the actual injector position.

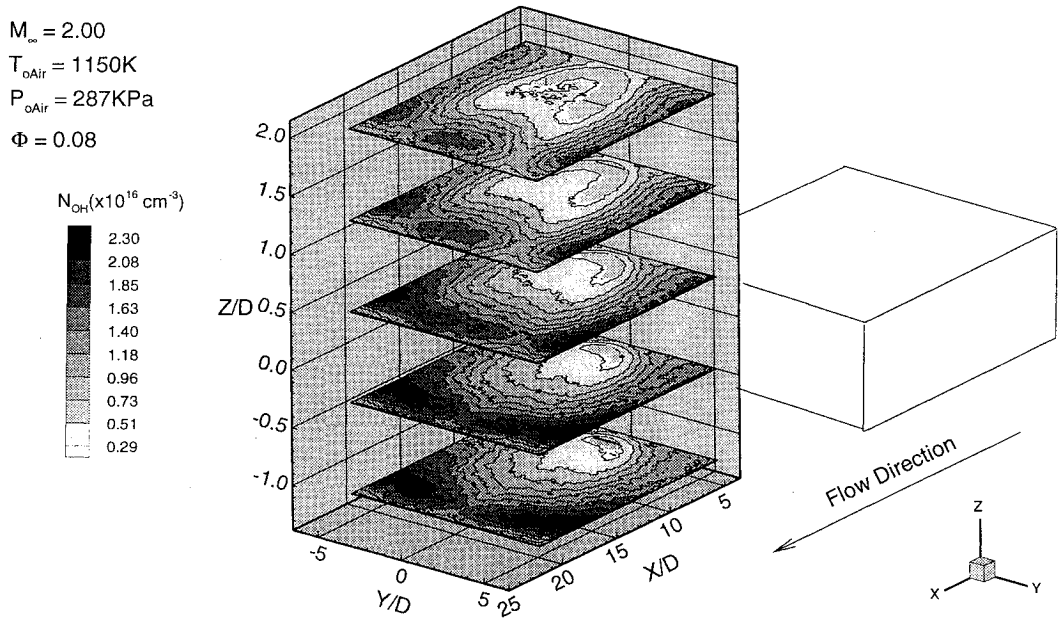

Fig. 4 Absolute OH concentration distributions for transverse H_2 injection behind a rearward-facing step. A schematic of the step was included for clarity and does not represent the actual scale.

The set of five OH density distribution images (Fig. 3) shows that for the unswept-ramp injection scheme the majority of the flame remains near the injector wall and along the centerline, extending no more than ~1.0 cm on either side of the centerline in the Y dimension. The region imaged shows very clearly the fuel plume denoted by the two pronounced lobes of flame at $Z/D = 2.0$ as it moves upwards into the freestream. Images at heights greater than $Z/D = 2.0$ show the two lobes merging together again, similar in appearance to the image of the $Z/D = -1.0$ plane and finally OH disappears at $Z/D \sim 6$. This indicates a nominally cylindrical flame envelope surrounding a core of fuel rich gas. Peak OH density values of approximately 5.4×10^{16} cm^{-3} were recorded in the most intense parts of the flame zone, quickly decreasing to a lower recorded limit of $\sim 4.5 \times 10^{15}$ cm^{-3} near the edge of the fuel plume.

For comparison, density distributions obtained previously[19] in a supersonic combustion flow behind a rearward-facing step with transverse H_2 injection are shown in Fig. 4. For these measurements air with a freestream Mach number $M_\infty = 2$ and stagnation temperature and pressure 1150 K and 287 kPa, respectively, entered the test section. The hydrogen was injected at a stagnation pressure of 335 kPa, stagnation temperature of 453 K, and a flow rate of 0.54 g/s. At this flow rate, the overall equivalence ratio was $\Phi = 0.08$. In this case, the H_2–air flame was much leaner than that of the unswept-ramp case with correspondingly lower peak OH concentrations of $\sim 2.6 \times 10^{16}$ cm^{-3}. The fuel plume, as in the previous set of images (Fig. 3), is clearly delineated by the region of reduced OH density. However, in this case significant OH density persists to large Z due to the increased fuel penetration produced by normal injection.

Apparent temperature distributions were obtained from time-averaged fluorescence intensities of five excitation lines. As stated earlier, using time-averaged fluorescence measurements to determine the temperature of highly intermittent reacting flows may introduce large systematic errors. However, the same time-averaged measurements are potentially an accurate method for obtaining the population density of individual rotational states, which in turn may be used to specify the average thermodynamical state of the probed species. Furthermore, by repeating the measurement for all of the rotational states of the probed species, the entire distribution can be mapped. Of course direct measurement of the population density of all of the rotational states of OH cannot be practically done. However, if it can be shown that the population distribution obtained by such time-averaged measurement behaves similarly to the population distribution of a thermodynamically equilibrated gas, then even two state population measurements may suffice to fully describe the entire rotational distribution.

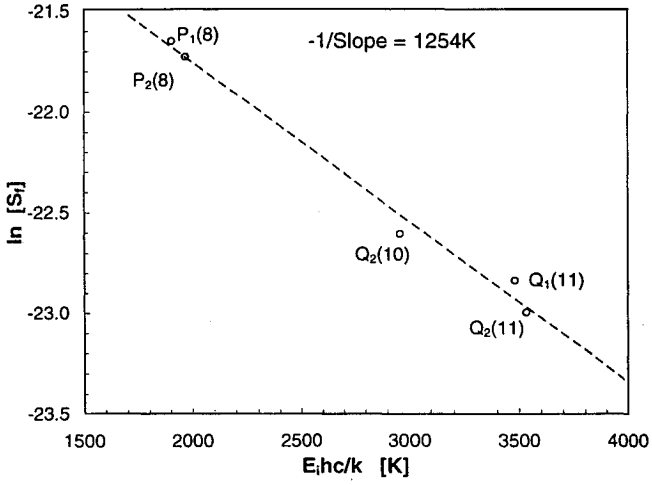

Fig. 5 Boltzmann plot of five time-averaged LIF measurements in an H_2–air supersonic combustion flow. The slope of $-1/T_{app}$ = 1245 K represents the apparent temperature at that point.

The existence of rotational equilibrium can be confirmed graphically by a Boltzmann plot. In this plot the detected fluorescence signal of each of the LIF emission lines S_i is corrected for predissociation of the emitting state P_i, for the absorption and emission rates B_i and A_i, respectively, and for the state degeneracy as follows:

$$S_f = \frac{S_i}{A_i B_i g_i / P_i} \tag{4}$$

The logarithm of this corrected signal S_f is then plotted against the energy of the absorbing state divided by the Boltzmann coefficient E_i/k. By combining Eqs. (1) and (2), it can be readily shown that at equilibrium, i.e., when Boltzmann distribution prevails, this semi-logarithmic plot must yield a straight line with a negative slope of $1/T$.

A Boltzmann plot of the time-averaged fluorescence measurement of five rotational transitions induced at a point in the flame is presented in Fig. 5. The experimental points in this figure appear to follow a straight line with a slope of $-1/T_{app}$, which suggests that although the intermittency is random, its average effect is similar for all lines. Similar Boltzmann plots obtained by LIF measurements of OH in an unperturbed atmospheric air furnace yielded a temperature

that was consistent within 3% of independent thermocouple measurements.[15] This good match confirms independently the accuracy of the reported[12,13] spectroscopic coefficients that were used to generate the Boltzmann plot in Fig. 5. Since the conditions in the furnace are steady, the same distribution is expected to be obtained there for single pulse measurements. By contrast, the flow in the combustion test section is highly intermittent and time-resolved measurements of the Boltzmann distribution are likely to fluctuate significantly. Nevertheless, the time-averaged Boltzmann plot for all of the points where the density of OH was sufficient for LIF measurements showed a well-established and reproducible Boltzmann distribution.

The apparent temperature T_{app} obtained from the Boltzmann distribution of Fig. 5 may not represent the true (gas-kinetic) time-averaged temperature at that point since the time-averaged fluorescence measurements are not correlated in this unsteady flow. Information regarding reaction rates, which are generally parameterized by the gas-kinetic temperature, cannot be inferred from T_{app}. However, Fig. 5 does establish a well-defined Boltzmann distribution of the time-averaged population among the rotational states of OH, and T_{app} is a valid measure of this distribution. For example, the specific rotational energy of OH obtained by summing the time-averaged product $N_{OHi}E_i/N_{OH}$ over all of the rotational states i is also the time-averaged specific internal energy e_{rot} of a rotationally fully excited diatomic molecular gas species in thermodynamic equilibrium[20] at the temperature T_{app}. Specifically this can be expressed by

$$e_{rot} = \bar{R}T_{app} \tag{5}$$

where $\bar{R}$ is the specific gas constant for OH. With this interpretation, T_{app} is a thermodynamic parameter that similarly to temperature specifies the time-averaged rotational energy of the probed species (note that T_{app} should not be confused with the rotational temperature of OH). At equilibrium, and with the ideal gas assumption, T_{app} may also be used to specify the specific internal energy and enthalpy of OH. Since a straight line with a specific slope could have been drawn using any pair of the measured state population densities, Fig. 5 also demonstrates that at the conditions of this experiment the slope of the Boltzmann plot, or T_{app}, can be determined by only two independent LIF measurements. Conversely, only two such LIF measurements can be considered independent with any pair fully specifying the apparent temperature. Specifying a time-averaged thermodynamic state by two such averaged quantities is comparable to specifying a momentary thermodynamic state by two simultaneous LIF measurements, from which the density and the true temperature are determined. For example, together with pressure, the average thermodynamic state of the OH within the volume element is fully specified by these averaged fluorescence measurements.

The error ΔT_{app} introduced by the measurement of the time-averaged LIF of only two lines can be calculated using the following exact differential of Eq. (3):

$$\frac{\Delta T_{app}}{T_{app}} = \frac{\Delta R}{R}\frac{kT}{\Delta E_{12}} \tag{6}$$

where $\Delta R/R$ is the uncertainty in the measurement of the fluorescence intensity ratio. Note that N_{OH1} and N_{OH2} do not contribute to this uncertainty if—as assumed here—their time-averaged values remain unchanged throughout the measurement. Since the measurement uncertainty of the population density of an individual state does not depend on an independent temperature measurement, the only error here is introduced by the calibration process, which in this experiment was <6%. Thus using the $P_1(8)$ and $Q_2(11)$ lines for this measurement the error is estimated to be $\Delta T_{app}/T_{app} = 9\%$.

The distribution of the apparent temperature was obtained from time-averaged fluorescence intensities of the following excitation lines: $P_1(8)$, $P_2(8)$, $Q_2(10)$, $Q_1(11)$, and $Q_2(11)$. Figure 6 presents the field of T_{app} in the $Z/D = 0.0$ plane. The image shows relatively small temperature variation even in regions where the OH concentration gradients are large. Thus, although the average OH density appears to vary significantly within the imaged plane, its specific time-averaged rotational energy and possibly its specific average enthalpy are uniformly distributed.

Ideally, the standard deviation of a measurement decreases as the number of samples is increased. To determine the effect of averaging of the LIF signal on the measurement of the apparent

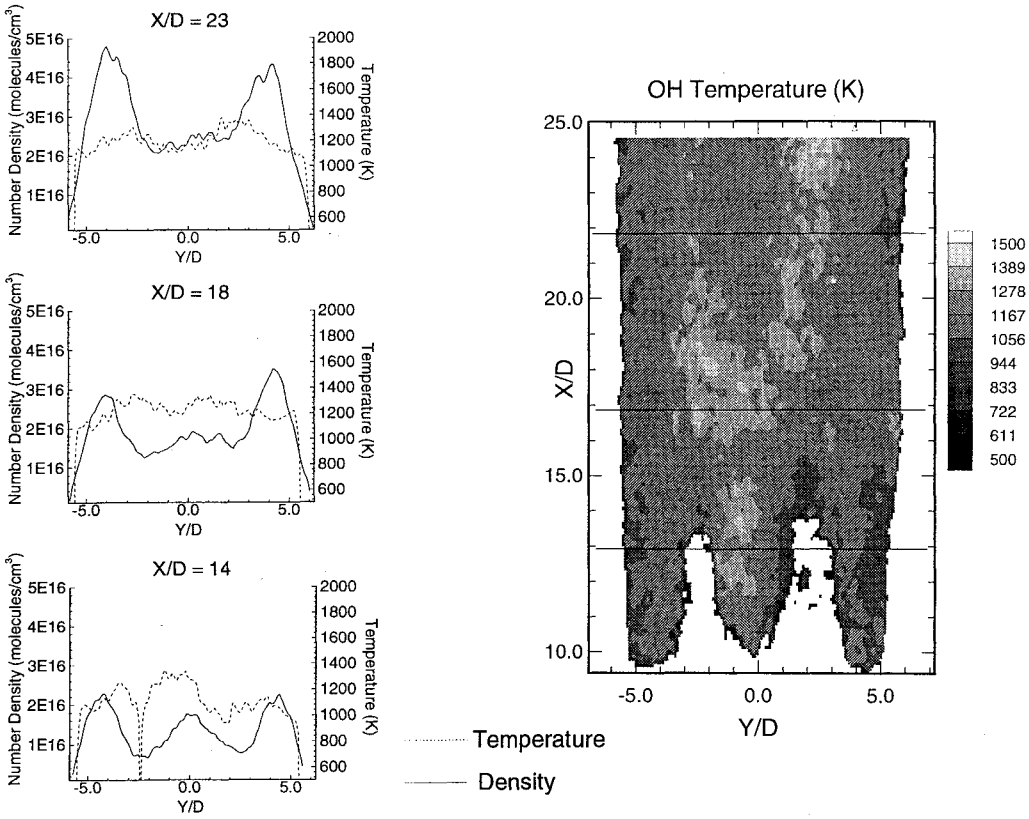

Fig. 6 Apparent temperature field at Z/D = 0.0 determined from average fluorescence images of five different rotational transitions of OH.

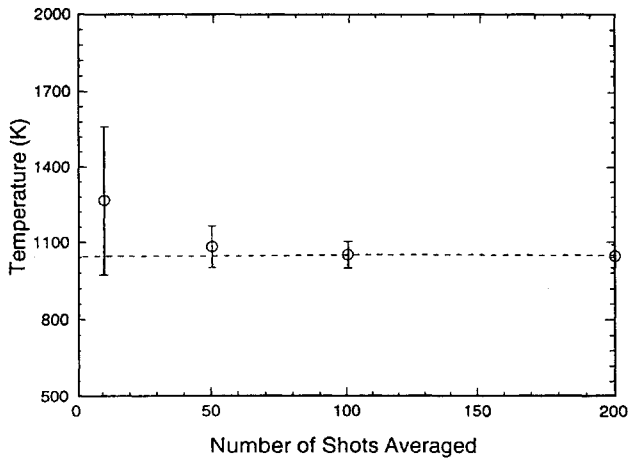

Fig. 7 Variation with sample size of the apparent temperature and its standard deviation at a point.

temperature, the standard deviation was computed for various sample sizes. Figure 7 shows a typical apparent temperature and associated standard deviation obtained from 10, 50, 100, and 200 shot averages at a single point in the flow. Although apparent temperatures obtained from these time-averaged measurements are comparable, the standard deviation appears to decrease rapidly with the sample size. Clearly, for the conditions of the present experiment, the advantage realized by averaging more than 100 samples was minimal.

Conclusions

PLIF images of OH density and apparent temperature in a supersonic combustion test section were produced using a tunable KrF laser. OH densities were obtained by the excitation of the $Q_2(11)$ ro-vibronic transition following calibration against a known OH concentration generated by the thermal dissociation of H_2O in an atmospheric air furnace. Peak OH concentrations of 5.4×10^{16} cm^{-3} were measured with an uncertainty of $\leq 21\%$. These results are consistent with previously measured densities[19] obtained in a leaner H_2–air environment, where peak OH concentrations were approximately 2.6×10^{16} cm^{-3}.

The turbulent fluctuations in the flame are expected to introduce systematic errors into nonsimultaneous, multiline temperature measurements. Thus, although measurements of the average temperature may not be possible by nonsimultaneous excitations, the linear dependance between the time-averaged fluorescence yield and the population density of any absorbing state allows the measurement of the time-averaged state population. Furthermore, results of the present experiment show that despite the flame intermittency the Boltzmann plot of the time-averaged LIF signal of five different rotational lines forms a straight line. Therefore, time-averaged measurements of the population density of any pair of rotational states should be sufficient to specify the population distribution within the entire rotational manifold of OH. Moreover, these two LIF measurements are valid presentation of two independent thermodynamic quantities such as the average density and the average specific rotational energy and therefore are a useful thermodynamic measurement that may be used for code validation.

Acknowledgments

This work was supported by the NASA Graduate Student Research Program Contract NGT-S0714 and by NASA Grant NAG-1-795 with G. Burton Northam as technical monitor.

References

[1]McDaniel, J., Fletcher, D., Hartfield, R., Jr., and Hollo, S., "Staged Transverse Injection into Mach 2 Flow Behind a Rearward-Facing Step: A 3-D Compressible Test Case for Hypersonic Combustor Code Validation," AIAA Paper 91-5071, Dec. 1991.

[2]Dyer, M. J., and Crosely, D. R., "Two-Dimensional Imaging of OH Laser-Induced Fluorescence in a Flame," *Optics Letters*, Vol. 7, Aug. 1982, pp. 382–384.

[3]Laufer, G., McKenzie, R. L., and Fletcher, D. G., "Method for Measuring Temperatures and Densities in Hypersonic Wind Tunnel Air Flows Using Laser-Induced O_2 Fluorescence," *Applied Optics*, Vol. 29, No. 33, 1990, pp. 4873–4883.

[4]Grieser, D. R., and Barnes, R. H., "Nitric Oxide Measurements in a Flame by Laser Fluorescence," *Applied Optics*, Vol. 19, No. 5, 1980, pp. 741–743.

[5]Chang, A. Y., Battles, B. E., and Hanson, R. K., "Simultaneous Measurements of Velocity, Temperature, and Pressure Using Rapid CW Wavelength-Modulation Laser-Induced Fluorescence of OH," *Optics Letters*, Vol. 15, No. 12, 1990, pp. 706–708.

[6]Allen, M. G., Parker, T. E., Reinecke, W. G., Legner, H. H., Foutter, R. R., Rawlins, W. T., and Davis, S. J., "Instantaneous Temperature and Concentration Imaging in Supersonic Air Flow Behind a Rear-Facing Step with Hydrogen Injection," AIAA Paper 92-0137, Jan. 1992.

[7]Seitzman, J. M., Hanson, R. K., DeBarber, P. A., and Hess, C. F., "Application of Quantitative Two-Line OH Planar Laser-Induced Fluorescence for Temporally Resolved Planar Thermometry in Reacting Flows," *Applied Optics*, Vol. 33, No. 18, 1994, pp. 4000–4012.

[8]Fletcher, D. G., "An Investigation of Nonsimultaneous Laser-Induced Fluorescence," AIAA Paper 93-0043, Jan. 1993.

[9]Palmer, J. L., and Hanson, R. K., "Single-Shot OH PLIF Thermometry in a Reacting Supersonic Free Jet," AIAA Paper 95-0517, Jan. 1995.

[10]Quagliaroli, T. M., Laufer, G., Krauss, R. H., and McDaniel, J. C., "Laser Selection Criteria for OH Fluorescence Measurements in Supersonic Combustion Test Facilities," *AIAA Journal*, Vol. 31, No. 3, 1993, pp. 520–527.

[11]Barlow, R. S., Dibble, R. W., and Lucht, R. P., "Simultaneous Measurement of Raman Scattering and Laser-Induced OH Fluorescence in Nonpremixed Turbulent Jet Flames," *Optics Letters*, Vol. 14, March 1989, pp. 263–265.

[12]Dimpfl, W. L., and Kinsey, J. L., "Radiative Lifetime of OH ($A^2\Sigma$) and Einstein Coefficients for the A-X System of OH and OD," *Journal of Quantitative Spectroscopy and Radiative Transfer*, Vol. 21, No. 3, 1979, pp. 233–241.

[13]Heard, D. E., Crosley, D. R., Jeffries, J. B., Smith, G. P., and Hirano, A., "Rotational Level Dependence of Predissociation in the $v' = 3$ Level of OH $A^2\Sigma^+$," *Journal of Chemical Physics*, Vol. 96, No. 6, 1992, pp. 4366–4371.

[14]Andresen, P., Bath, A., Gröger, W., Lülf, H. W., Meijer, G., and ter Meulen, J. J., "Laser-Induced Fluorescence with Tunable Excimer Lasers as a Possible Method for Instantaneous Temperature Field Measurements at High Pressures: Checks with an Atmospheric Flame," *Applied Optics*, Vol. 27, No. 2, 1988, pp. 365–378.

[15]Grinstead, J. H., Laufer, G., and Krauss, R. H., "Calibration Source for OH Laser-Induced Fluorescence Density Measurements Using Thermally Dissociated H_2O in Atmospheric Air," *Applied Optics*, Vol. 33, No. 6, 1994, pp. 1115–1119.

[16]Krauss, R. H., and McDaniel, J. C., Jr., "A Clean Air Continuous Flow Propulsion Facility," AIAA Paper 92-3912, July 1992.

[17]Kohse-Höinghaus, K., Jeffries, J. B., Copeland, R. A., Smith, G. P., and Crosley, D. R., "The Quantitative LIF Determination of OH Concentrations in Low-Pressure Flames," *Twenty-Second Symposium (International) on Combustion*, Combustion Inst., Pittsburgh, PA, 1988, pp. 1857–1866.

[18]Copeland, R. A., Wise, M. L., and Crosley, D. R., "Vibrational Energy Transfer and Quenching of OH($A^2\Sigma^+$, $v' = 1$)," *Journal of Chemical Physics*, Vol. 92, No. 20, 1988, pp. 5710–5717.

[19]Quagliaroli, T. M., Laufer, G., Krauss, R. H., and McDaniel, J. C., Jr., "Planar Measurement of Absolute OH Number Density Distributions in a Supersonic Combustion Tunnel," *Journal of Propulsion and Power*, Vol. 11, No. 5, 1995, pp. 1083–1086.

[20]Vincenti, W. G., and Kruger, C. H., Jr., *Introduction to Physical Gas Dynamics*, Krieger, Malabar, FL, 1986, p. 133.